

Effects of Composition and Matrix Polarity on Network Development in Organogels of Poly(ethylene glycol) and Dibenzylidene Sorbitol

Elizabeth A. Wilder,[†] Carol K. Hall,[†] Saad A. Khan,[†] and Richard J. Spontak^{*,†,‡}

Departments of Chemical Engineering and Materials Science & Engineering,
North Carolina State University, Raleigh, North Carolina 27695

Received December 30, 2002. In Final Form: April 9, 2003

Dibenzylidene sorbitol (DBS) is a low-molecular-weight organic molecule that can gel a variety of organic solvents and polymers by self-organizing into a three-dimensional nanofibrillar network through hydrogen-bonding and phenyl interactions. In this work, we investigate the composition dependence of such “organogels” prepared with poly(ethylene glycol) (PEG) and two PEG derivatives differing in methoxy end-group substitution, which serves to reduce matrix polarity. Transmission electron microscopy reveals that individual DBS nanofibrils measure from about 10 to 70 nm in diameter, with a primary nanofibrillar diameter of about 10 nm. Dynamic rheological measurements indicate that the rate by which the elastic modulus increases during gelation, the temperatures corresponding to gel formation and dissolution, and the magnitude of the elastic modulus are all sensitive to the DBS mass concentration (ϕ) and the matrix polarity. Hydroxy-end-capped PEG/DBS systems gel more slowly, but dissolve faster, than their methoxy-end-capped analogues at constant ϕ . The elastic modulus, however, is less dependent on matrix polarity and scales as $\phi^{1.8}$ over the range of ϕ examined in PEG/DBS organogels. Time–temperature superposition analysis provides direct evidence for the activation energy of network evolution increasing linearly with (i) decreasing ϕ at constant matrix polarity and (ii) increasing matrix polarity at constant ϕ .

Introduction

Physical gels are generally produced when a minor component in a liquid solution forms a three-dimensional elastic network through microphase separation or specific intermolecular interactions that include hydrogen bonds or electrostatic interactions, the strength of which typically measures on the order of 20 kJ/mol.¹ Such networks are commonly disrupted upon heating, but re-form during cooling, to exhibit thermoreversibility. In addition, physical gel networks are often thixotropic in nature, since they likewise collapse if sufficiently deformed but recover upon quiescence.^{2,3} If the solvent molecules are organic, then we refer to such physical gels as “organogels”, which have recently become the subject of increasing fundamental and technological interest.^{4–12} These fascinating materials are readily generated at experimentally accessible conditions by dissolving a small amount of the gelling agent,

also referred to as gelator or, more recently, tecton,¹³ in an organic solvent at elevated temperatures. Upon cooling, the gelator molecules self-organize into colloidal aggregates that link together in a nanoscale network capable of (i) restraining the matrix molecules through molecular capillary forces or surface tension^{8,14} and (ii) imparting the system with solid-like rheological properties.

Organic species with active functionalities capable of promoting sufficient intermolecular interaction to elicit molecular self-assembly are often suitable as gelators. Sugar-based gelators are ubiquitous in numerous technologies and include 1,3:2,4-dibenzylidene sorbitol,^{2,3,10,11,14–31} the subject of the present work, as well

* To whom correspondence should be addressed. E-mail: rich_spontak@ncsu.edu.

[†] Department of Chemical Engineering.

[‡] Department of Materials Science & Engineering.

(1) Atkins, P. W. *Physical Chemistry*, 5th ed.; Freeman: New York, 1994.

(2) Fahländer, M.; Fuchs, K.; Friedrich, C. *J. Rheol.* **2000**, *44*, 1103.

(3) Kobayashi, T.; Hasegawa, H.; Hashimoto, T. *Hihon Reoraji Gakkaishi* **1989**, *17*, 155.

(4) Amanokura, N.; Yoza, K.; Shinmori, H.; Shinkai, S.; Reinhoudt, D. N. *J. Chem. Soc., Perkin Trans. 2* **1998**, 2585.

(5) Amanokura, N.; Kanekiyo, Y.; Shinkai, S.; Reinhoudt, D. N. *J. Chem. Soc., Perkin Trans. 2* **1999**, 1995.

(6) Geiger, C.; Stanescu, M.; Chen, L.; Whitten, D. G. *Langmuir* **1995**, *11*, 2241.

(7) Hanabusa, K.; Maesaka, Y.; Kimura, M.; Shirai, H. *Tetrahedron Lett.* **1999**, *40*, 2385.

(8) Duncan, D. C.; Whitten, D. G. *Langmuir* **2000**, *16*, 6445.

(9) Bauer, T.; Thomann, R.; Mülhaupt, R. *Macromolecules* **1998**, *31*, 7651.

(10) Watase, M.; Nakatani, Y.; Itagaki, H. *J. Phys. Chem. B* **1999**, *103*, 2366.

(11) Terech, P.; Weiss, R. G. *Chem. Rev.* **1997**, *97*, 3133.

(12) Abdallah, D. J.; Weiss, R. G. *Adv. Mater.* **2000**, *12*, 1237.

(13) Fuchs, K.; Bauer, T.; Thomann, R.; Wang, C.; Friedrich, C.; Mülhaupt, R. *Macromolecules* **1999**, *32*, 8404.

(14) Nahir, T. M.; Qui, Y.-J.; Williams, J. L. *Electroanalysis* **1994**, *6*, 972.

(15) Mercurio, D. J.; Spontak, R. J. *J. Phys. Chem. B* **2001**, *105*, 2091.

(16) Mercurio, D. J.; Khan, S. A.; Spontak, R. J. *Rheol. Acta* **2001**, *40*, 30.

(17) Nuñez, C. M.; Whitfield, J. K.; Mercurio, D. J.; Ilzhoefer, J. R.; Spontak, R. J. *Macromol. Symp.* **1996**, *106*, 275.

(18) Thierry, A.; Fillon, B.; Straupé, C.; Lotz, B.; Wittmann, J. C. *Prog. Colloid Polym. Sci.* **1992**, *87*, 28.

(19) Janssen, R. H. C.; Stümpflen, V.; van Bortel, M. C. W.; Bastiaansen, C. W. M.; Broer, D. J.; Tervoort, T. A.; Smith, P. *Macromol. Symp.* **2000**, *154*, 117.

(20) Janssen, R. H. C.; Stümpflen, V.; Bastiaansen, C. W. M.; Broer, D. J.; Tervoort, T. A.; Smith, P. *Jpn. J. Appl. Phys.* **2000**, *39*, 2721.

(21) Schamper, T.; Jablon, M.; Randhawa, M. H.; Senatore, A.; Warren, J. D. *J. Soc. Cosmet. Chem.* **1986**, *37*, 225.

(22) Thomas, P.; Sibi, S. *Comptes Rendus* **1926**, *183*, 282.

(23) Thierry, A.; Straupé, C.; Lotz, B.; Wittmann, J. C. *Polym. Commun.* **1990**, *31*, 299.

(24) Yamasaki, S.; Tsutsumi, H. *Bull. Chem. Soc. Jpn.* **1994**, *67*, 906.

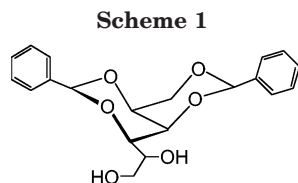
(25) Yamasaki, S.; Tsutsumi, H. *Bull. Chem. Soc. Jpn.* **1994**, *67*, 2053.

(26) Yamasaki, S.; Tsutsumi, H. *Bull. Chem. Soc. Jpn.* **1995**, *68*, 123.

(27) Yamasaki, S.; Ohashi, Y.; Tsutsumi, H.; Tsujii, K. *Bull. Chem. Soc. Jpn.* **1995**, *68*, 146.

(28) Watase, M.; Itagaki, H. *Bull. Chem. Soc. Jpn.* **1998**, *71*, 1457.

(29) Ilzhoefer, J. R.; Broom, B. C.; Nepa, S. M.; Vogler, E. A.; Khan, S. A.; Spontak, R. J. *J. Phys. Chem.* **1995**, *99*, 12069.



as sorbitol derivatives possessing *p*-nitrophenyl⁴ or *p*-aminophenyl⁵ groups. Alternatively, gelators may also be synthesized from cholesterol compounds^{6,8,32} or contain complex anthracenyl functionalities.³² Hanabusa et al.^{7,33} have reported on the gelation effectiveness of 2-amino-2-phenylethanol, *n*-benzyloxycarbonyl-L-alanine 4-hexadecanoyl-2-nitrophenyl ester, and related compounds, whereas other gelators under current consideration are derived from barbituates and 2,4,6-triaminopyrimidines,^{9,13} as well as from 12-hydroxyoctadecanoic acids^{34–36} and 12-hydroxystearates.^{37,38} Weiss and co-workers^{11,12} have recently provided extensive reviews on the emerging subject of organogels and systematically described a broad spectrum of low-molecular-mass organic gelators (LMOGs) and their potential commercial applications. While a wide variety of organic gelators have been identified and successfully used to produce stable organogels, the prerequisites for a gelator in terms of chemical functionality are commonly encountered in many organic molecules, in which case numerous gelators may remain unknown at the present time.³²

Dibenzylidene sorbitol (DBS, Scheme 1) constitutes an excellent example of a low-molecular-weight organic molecule that can self-organize into nanoscale fibrils typically measuring from 10 nm to 0.8 μ m in diameter through a combination of hydrogen-bonding and phenyl interactions. At sufficiently high DBS concentrations, the nanoscale fibrils form a percolated network that consequently promotes gelation of various organic solvents and polymers. Organogels produced in this fashion have attracted commercial interest due to their many possible applications in cosmetics, personal care products, biomedical materials, and (opto)electronic devices. Dibenzylidene sorbitol is a derivative of the natural sugar alcohol D-glucitol²⁸ and can be synthesized by a condensation reaction between benzaldehyde and sorbitol.³⁹ In its native state, DBS exists as a crystalline solid with a melting point of about 220–225 °C.^{2,40} The amphiphilic DBS molecule is often described as “butterfly-like” with a sorbitol body and two benzylidene wings. The hydrophobic phenyl rings facilitate DBS dissolution in a wide variety of organic solvents¹⁸ and, in combination with its acetal oxygens and pendant hydroxyl groups, endow DBS with its unique ability to self-organize into nanofibrils and

ultimately induce gelation. Since the discovery of DBS in the late 1800s by Meunier,⁴¹ numerous studies^{21,23,25–28,30} have sought to elucidate the gelation efficacy of DBS in simple, low-molar-mass organic solvents.

More recent efforts have extended the use of DBS as a gelator to more complex systems, such as those composed of macromolecules and mesomorphous molecules. Thus far, evidence of DBS-induced physical gelation has been reported for isotactic polypropylene (iPP),³ poly(propylene glycol) (PPG),^{2,15,16} silicone fluids⁴² (including block copolymers derived therefrom^{29,43}), and small-molecule liquid crystals.^{19,20} Since DBS can promote gelation in organic media at concentrations as low as 0.1 wt %, ²³ it is particularly attractive for processes and applications that require the uncompromised physical and/or chemical properties of a liquid or polymer melt in a thermally reversible elastic solid. Moreover, DBS can likewise be used to modify the matrix of glassy⁴⁴ and semicrystalline^{18,39,45–60} polymers. To identify the material and environmental factors governing the molecular self-organization of DBS, several efforts have been directed toward examining the morphological characteristics and rheological properties of macromolecular organogels produced with DBS. The DBS nanofibrils and nanofibrillar network observed^{24,26} in organogels derived from low-molar-mass organic solvents have also been detected in macromolecular organogels. Rheological studies of DBS in iPP,³ PPG,^{2,15,16} and silicones⁴² have together shown that the elastic-like character of these materials depends on factors such as composition, molecular weight, temperature, and extent of deformation.

Although the recent surge of interest in organogels has certainly improved the understanding of gelators such as DBS and their ability to self-organize into three-dimensional network structures, the molecular interactions governing gelation and gel elasticity remain ambiguous. Specifically, the extent to which DBS molecules interact with matrix molecules (or segments, as in the case of macromolecules) has not been clearly addressed. While studies¹⁰ have suggested that solvent molecules are not assimilated within the DBS nanofibrillar network, it nonetheless remains possible that matrix molecules interact with DBS during gelation and affect the process

(30) McKenna, G. B.; Kern, F.; Candau, S. J.; Wittmann, J. C.; Thierry, A. *Abstr. Am. Chem. Soc.* **1991**, 202, 201.

(31) Silva, F.; Sousa, M. J.; Pereira, C. M. *Electrochim. Acta* **1997**, 42, 3095.

(32) Lin, Y.-C.; Kachar, B.; Weiss, R. G. *J. Am. Chem. Soc.* **1989**, 111, 5542.

(33) Hanabusa, K.; Okui, K.; Karaki, K.; Kimura, M.; Shirai, H. *J. Colloid Interface Sci.* **1997**, 195, 86.

(34) Tachibana, T.; Mori, T.; Hori, K. *Bull. Chem. Soc. Jpn.* **1980**, 53, 1714.

(35) Tachibana, T.; Mori, T.; Hori, K. *Bull. Chem. Soc. Jpn.* **1981**, 54, 73.

(36) Tachibana, T.; Kayama, K.; Takeno, H. *Bull. Chem. Soc. Jpn.* **1972**, 45, 415.

(37) Tachibana, T.; Kambara, H. *Bull. Chem. Soc. Jpn.* **1969**, 42, 3422.

(38) Tachibana, T.; Kitazawa, S.; Takeno, H. *Bull. Chem. Soc. Jpn.* **1970**, 43, 2418.

(39) Sterzynski, R.; Lambla, M.; Crozier, H. *Adv. Polym. Technol.* **1994**, 13, 25.

(40) Angyal, S. J.; Lawler, J. V. *J. Am. Chem. Soc.* **1944**, 66, 837.

(41) Meunier, M. *J. Ann. Chim. Phys.* **1891**, 22, 412.

(42) Smith, J. M.; Katsoulis, D. E. *J. Mater. Chem.* **1995**, 5, 1899.

(43) Ilzhoefer, J. R.; Spontak, R. J. *Langmuir* **1995**, 11, 3288.

(44) Wilder, E. A. Ph.D. Dissertation, North Carolina State University, 2003.

(45) Mitra, D.; Misra, A. *J. Appl. Polym. Sci.* **1988**, 36, 387.

(46) Mitra, D.; Misra, A. *Polymer* **1988**, 29, 1990.

(47) Cooke, J. *Plast. Compd.* **1990**, 13, 30.

(48) Fujiyama, M.; Wakino, T. *J. Appl. Polym. Sci.* **1991**, 42, 2749.

(49) Fujiyama, M.; Wakino, T. *J. Appl. Polym. Sci.* **1991**, 42, 2739.

(50) Kim, C. Y.; Kim, Y. C. *Polym. Eng. Sci.* **1993**, 33, 1445.

(51) Smith, T. L.; Masilamani, D.; Bui, L. K.; Khanna, Y. P.; Bray, R. G.; Hammond, W. B.; Curran, S.; Belles, J. J.; Binder-Castelli, S. *Macromolecules* **1994**, 27, 3147.

(52) Smith, T. L.; Masilamani, D.; Bui, L. K.; Brambilla, R.; Khanna, Y. P.; Gabriel, K. A. *J. Appl. Polym. Sci.* **1994**, 52, 591.

(53) Dolgopolsky, I.; Silberman, A.; Kenig, S. *Polym. Adv. Technol.* **1995**, 6, 653.

(54) Feng, Y.; Jin, X.; Hay, J. N. *J. Appl. Polym. Sci.* **1998**, 69, 2089.

(55) Nagarajan, K.; Levon, K.; Myerson, A. S. *J. Therm. Anal. Calorim.* **2000**, 59, 497.

(56) Garg, S. N.; Stein, R. S.; Su, T. K.; Tabar, R. J.; Misra, A. In *Kinetics of Aggregation and Gelation*; Family, F., Landau, D. P., Eds.; Elsevier: New York, 1984; pp 229–234.

(57) Shepard, T. A.; DelSorbo, C. R.; Louth, R. M.; Walborn, J. L.; Norman, D. A.; Harvey, N. G.; Spontak, R. J. *J. Polym. Sci. B: Polym. Phys.* **1997**, 35, 2617.

(58) Hoffmann, K.; Huber, G.; Mader, D. *Macromol. Symp.* **2001**, 176, 83.

(59) Nagarajan, K.; Myerson, A. S. *Cryst. Growth Des.* **2000**, 1, 131.

(60) Marco, C.; Ellis, G.; Gomez, M. A.; Arribas, G. M. *J. Thermal Anal. Calorim.* **2002**, 68, 61.

or product. In this work, the roles of polymer composition and polarity on organogel development are simultaneously investigated through the combined use of a low-molecular-weight liquid polymer and two of its chemically modified derivatives.

Experimental Section

Materials. Dibenzylidene sorbitol samples were provided by Milliken Chemicals (Spartanburg, SC) and used as-received. Three grades of liquid poly(ethylene glycol) (PEG) differing slightly in number-average molecular weight ($\bar{M}_n = 200, 300$, and 400), as well as a methoxy-endcapped PEG (PEGme, $\bar{M}_n = 350$) and a dimethoxy-endcapped PEG (PEGdme, $\bar{M}_n = 250$), were purchased from Aldrich Chemicals (St. Louis, MO) and used without further purification.

Methods. Organogels were prepared by dissolving a predetermined amount of DBS in a given polymer on a hot plate maintained at 200 °C. After 10 min of constant agitation at 200 rpm, the solution was removed from the hot plate and allowed to cool quiescently. Resultant organogels were analyzed approximately 1 week later. Specimens of the PEG/DBS systems for analysis by transmission electron microscopy (TEM) were produced via two different routes. A nongelled solution with 0.5 wt % DBS was dripped from a micropipet onto a carbon-supported TEM grid and washed repeatedly with toluene to remove residual PEG. Organogels were cut by hand into thin slices with a razor blade and soaked in distilled water for a period of about 2 weeks to leach out the PEG. The remaining (insoluble) DBS network was carefully picked up on carbon-supported TEM grids and likewise washed repeatedly with toluene. The grids were examined with and without exposure to the vapor of RuO₄(aq), which selectively stains the phenyl rings of DBS,⁵⁷ in a Zeiss EM902 electron spectroscopic microscope operated at an accelerating voltage of 80 kV and energy-loss (ΔE) settings of either 0 or 150 eV. Images were acquired on negative plates and digitized at 600 dpi for analysis and presentation purposes. Dynamic rheological tests were performed on two rheometers: a Rheometrics mechanical spectrometer (RMS-800) and a Rheometrics dynamic stress rheometer (DSR). A parallel-plate geometry with 25 mm plates (serrated, when appropriate) and a gap size of 1–2 mm, depending on the experiment, was used throughout this study. Frequency (ω) spectra of the elastic (G') and viscous (G'') moduli were collected at strain amplitudes of less than 1.5% in the linear viscoelastic limit.

Results and Discussion

Before examining the morphological characteristics and rheological properties of the DBS organogels produced here, we briefly consider the chemical effects of methoxy termination on PEG. One convenient measure used to predict the solubility of one component in another is the solubility parameter (δ) based on the cohesive energy density. Since the three PEG grades and two PEG derivatives used in this work are all soluble in common organic solvents, δ can be quickly and crudely estimated. A more accurate and systematic method by which to ascertain differences in δ due to molecular weight and termination relies on the use of group contribution methods (GCMs). Several GCMs are available for this purpose, and we elect to use the method of Hoftyzer and van Krevelen⁶¹ (inclusive of polar and hydrogen-bonding contributions) in our calculation. If n denotes the number of CH₂CH₂O repeat units per polymer molecule, then the calculated values of δ are 19.8 J^{1/2}/cm^{3/2} for PEGme ($n = 7$) and 19.5 J^{1/2}/cm^{3/2} for PEGdme ($n = 5$) and range from 21.5 to 23.6 J^{1/2}/cm^{3/2} for the three PEG grades ($n = 4, 7$, and 9). From a thermodynamic analysis of gel formation temperatures and solubility considerations, Fahrlander et al.² report that δ for DBS (as measured in PPG, although

the solvent should be inconsequential) is about 23.9 J^{1/2}/cm^{3/2}. Thus, we anticipate that DBS will be marginally more soluble in PEG than in PEGme or PEGdme.

The principal difference between PEG and its two derivatives lies in hydroxy (or methoxy) termination. Our reason for varying the chemical identity of the PEG termination is to explore the possibility that DBS molecules can interact with hydroxy-terminated PEG and that such interaction may affect gelation or network elasticity. This hypothesis is supported by the previous findings of Raghavan et al.,⁶² who reported that PEG termination influences the network-forming efficacy of another class of physical gels, namely, organic–inorganic gels based on silica. A parameter that would describe the magnitude of this effect is the number density of hydroxyl groups (ϵ), given by

$$\epsilon = \frac{n_{\text{OH}} N_A \rho}{\bar{M}_n} \quad (1)$$

where n_{OH} is the number of hydroxyl groups per molecule, N_A is Avogadro's number, and ρ represents mass density. Values of ρ (in g/cm³) are 1.13 for PEG (independent of n), 1.09 for PEGme, and 1.03 for PEGdme, according to the manufacturer, in which case corresponding values of ϵ (in hydroxyl groups/nm³) are 4.5 for PEG ($\bar{M}_n = 300$), 1.9 for PEGme, and 0.0 for PEGdme. While the variation in these ϵ with respect to n_{OH} is not exactly linear, the linear correlation coefficient (0.995) confirms reasonably good linearity. Since such minor deviation is within the accuracy of the \bar{M}_n measurements, the results obtained here for PEG, PEGme, and PEGdme can be systematically compared directly in terms of the number of hydroxyl end groups (n_{OH}) on each.

Gel Morphology. Morphological studies^{23,24,26} of self-organized DBS in low-molar-mass solvents indicate that the nanofibrillar diameter typically ranges from 10 nm to 0.8 μm . Thierry et al.²³ have shown that the nanofibrils formed in tetrahydrofuran/benzene solutions can grow very long and exhibit surprisingly few branch points. In marked contrast, the electron micrographs provided by Ilzhoefer and Spontak^{29,43} and Smith and Katsoulis⁴² clearly reveal that the DBS networks generated in silicone polymers consist of slightly thicker nanofibrils and appear highly connected and branched. Both morphologies are observed in the present work. Parts a and b of Figure 1 are energy-filtered TEM images obtained at $\Delta E = 0$ eV from an unstained specimen of a PEG/DBS organogel prepared with 7 wt % DBS. Both images display DBS nanofibrils that tend to measure between ~ 10 and 70 nm in diameter, which is consistent with nanofibrillar measurements performed on iPP/DBS⁵⁷ and PPG/DBS¹⁵ systems. Note that the nanofibrils in these images are moderately branched, unlike the long, discrete nanofibrils reported elsewhere²³ and observed sporadically in the present specimen. Some of the thick nanofibrils in Figure 1b may represent bundles of nanofibrils that either never fully dissolved during gel preparation or aggregated upon gelation, as discussed elsewhere.⁵⁷ While the nanofibrils evident in Figure 1a and b provide close examination of self-organized DBS nanofibrils, they are not representative of the gel network morphology at this DBS concentration. Indeed, the image presented in Figure 1c identifies a more characteristic portion of the same PEG/DBS organogel that appears highly interconnected and branched, in

(61) van Krevelen, D. W. *Properties of Polymers*, 3rd ed.; Elsevier: New York, 1997.

(62) Raghavan, S. R.; Walls, H. J.; Khan, S. A. *Langmuir* **2000**, *16*, 7920.

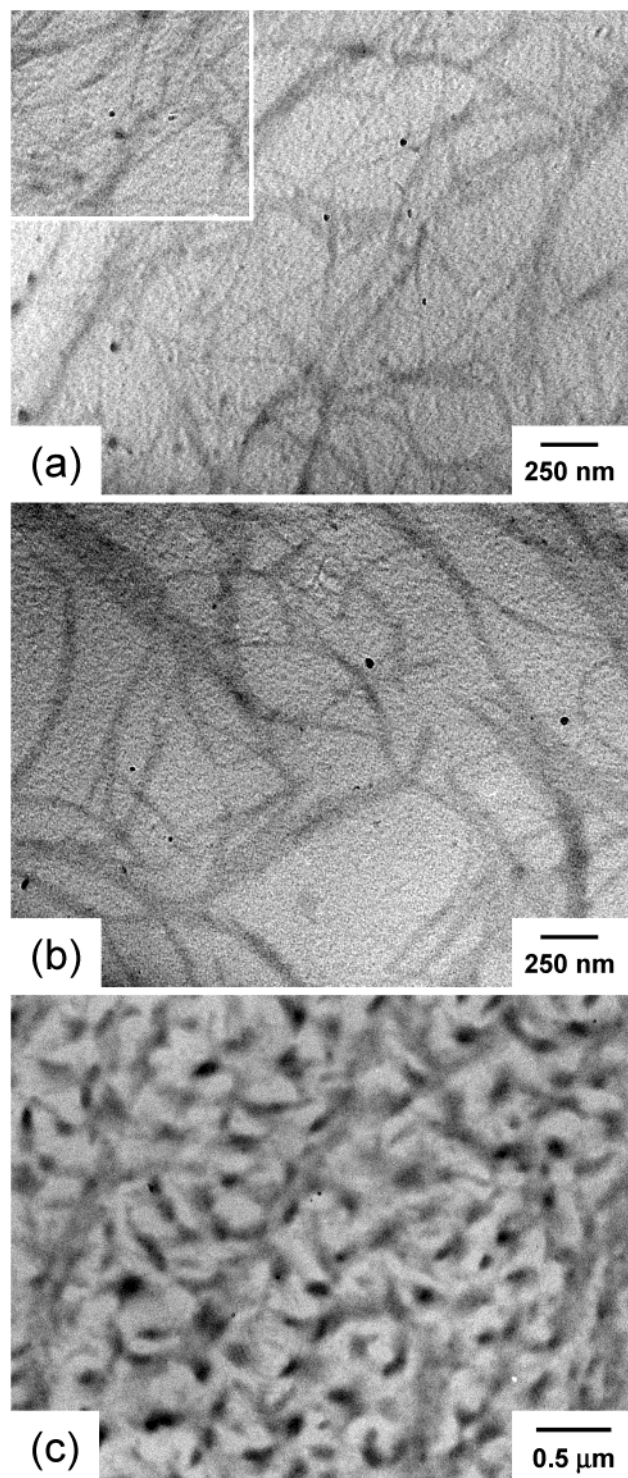


Figure 1. Zero-loss energy-filtered TEM images of a PEG/DBS organogel with 7 wt % DBS in which the PEG was removed by solvent extraction in water, followed by dissolution in toluene. The images in parts a and b display individual nanofibrils and nanofibrillar bundles, whereas the micrograph in part c shows a more highly connected network that is representative of this concentrated organogel.

agreement with intuitive expectation for a highly concentrated organogel. In this case, the diameter of the nanofibrils comprising the network cannot be ascertained with certainty due to superpositioning of the 3D network along the projection axis.

A gallery of energy-filtered TEM images in which the DBS molecules in PEG/DBS organogels are selectively

stained with the vapor of $\text{RuO}_4(\text{aq})$ is provided in Figure 2. The inset presented in Figure 2a displays a feature in a PEG/DBS system with 0.5 wt % DBS that appears as a central site from which nanofibrils measuring about 10 nm in diameter extend radially. Features of this type are strikingly reminiscent of nucleation sites and suggest that network formation occurs via a nucleation and growth mechanism. We shall return to this topic in subsequent sections. Figure 2a shows a network in a 7.0 wt % DBS organogel and appears qualitatively similar to the micrographs presented in Figure 1a and b. Most of the densely stained nanofibrils evident in Figure 2a measure between 20 and 40 nm in diameter. Close examination of this image reveals the existence of finer nanofibrils, which are more clearly visible in the higher-magnification image provided in Figure 2b. An intricately connected network is evident in this image, as well as in the complementary images obtained at 0 eV (zero-loss imaging) in Figure 2c and 150 eV (contrast-sensitive imaging) in Figure 2d. The fine nanofibrils are only peripherally stained and measure between 9 and 15 nm across, whereas the large nanofibrils appear to consist of several fine nanofibrils. Such nanofibrillar coordination may explain the wide variation in nanofibrillar diameters reported in the literature and supports the existence of a “primary” nanofibril, which measures 9–10 nm in diameter for DBS.

The observation that the RuO_4 stains only the periphery of the nanofibrils in Figure 2 is surprising, since this compound is expected to react with the phenyl rings of the DBS molecules. We offer three possible scenarios to explain this observation. In the first, residual PEG is located along the surface of the nanofibrils due to either incomplete removal or chemical attachment. Previous efforts have shown¹⁵ that DBS nanofibrils in PPG do not stain as quickly as the polyether molecules, in which case RuO_4 may serve as a negative, rather than positive, stain for PEG-embedded DBS nanofibrils. No evidence exists, however, to corroborate the existence of residual PEG in any of the specimens prepared here. Another explanation contends that peripheral staining occurs because RuO_4 molecules do not penetrate into the core of the nanofibrils, indicating that the phenyl rings of the DBS molecules are packed closely together in registry. This scenario is consistent with recent X-ray data¹⁵ that suggest nanofibrillar, as well as bulk, DBS is crystalline. A third possibility is that the nanofibrils are, in fact, hollow. This last scenario is intriguing, since it would also explain the discrepancy in size between the DBS molecule, which measures about 1.3 nm across in an outstretched conformation (see Scheme 1), and the primary nanofibril, which is about 9–10 nm in diameter. While each of these explanations may help to elucidate the mechanism of DBS self-organization, we must point out that (i) they cannot be differentiated from the data in Figure 2 and (ii) more than one of these scenarios may be simultaneously responsible for the images reported here.

Gel Formation and Dissolution. Fahrlander et al.² and Mercurio et al.¹⁶ have both demonstrated that DBS network formation in PPG depends sensitively on organogel composition and PPG molecular weight, the latter of which relates to solubility or, alternatively, solvent polarity. In this vein, Figure 3a illustrates the effect of DBS concentration on gelation kinetics in PEG/DBS organogels composed of PEG with $\bar{M}_n = 300$. Since the difference in molecular weight among the three PEG homopolymers examined does not measurably affect the rheological properties of the organogels, the PEG with $\bar{M}_n = 300$ will be used in nearly all the tests reported here, unless otherwise noted. Figure 3a shows the time-

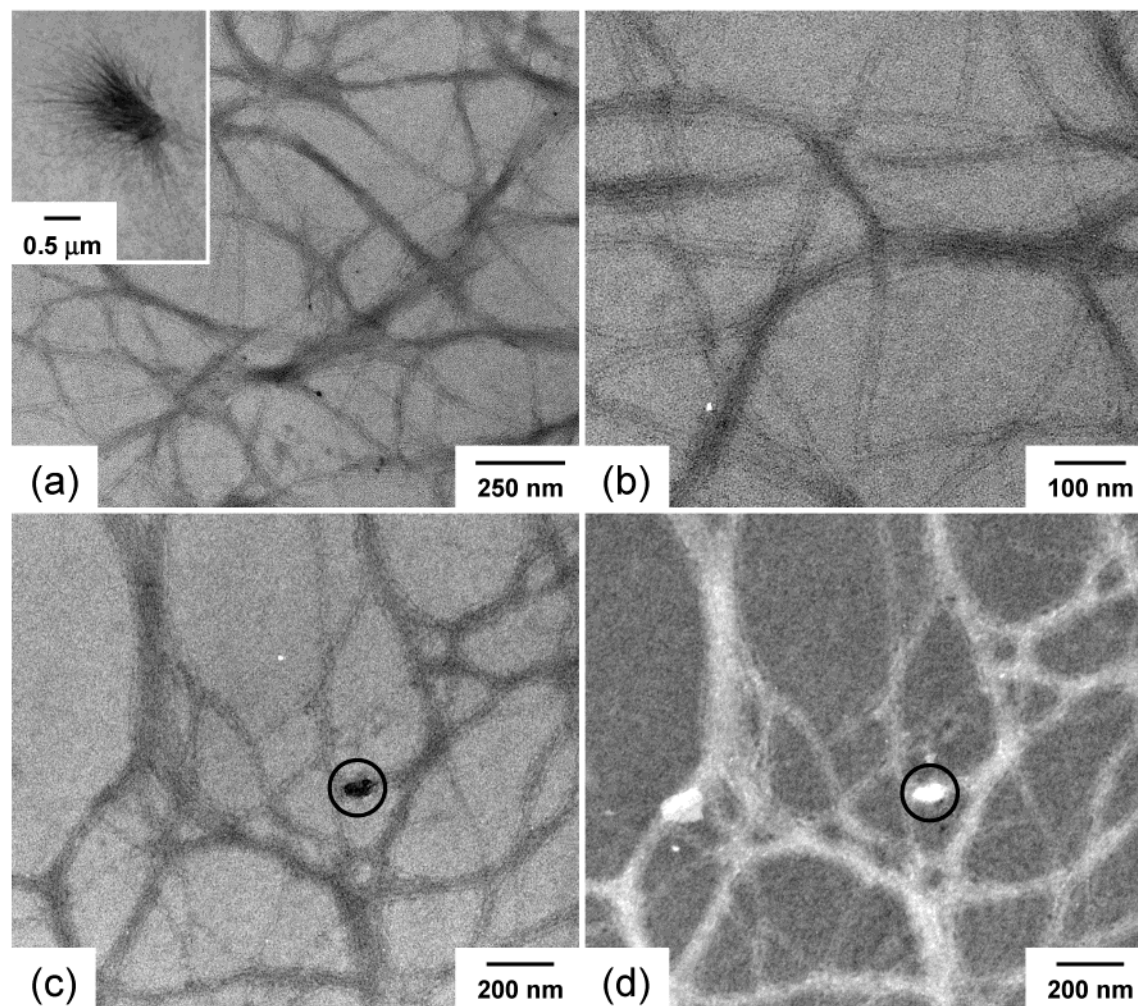


Figure 2. Energy-filtered TEM images of a PEG/DBS organogel with 7 wt % DBS in which the PEG was removed by solvent extraction in water, followed by dissolution in toluene and selective staining with the vapor of $\text{RuO}_4(\text{aq})$. The zero-loss image in part a displays a nanofibrillar network that is grossly similar to those in Figure 1. Close examination of part a and the enlargement in part b reveals the existence of fine (“primary”) nanofibrils that measure 9–10 nm in diameter. The images in parts c and d are complementary zero-loss ($\Delta E = 0$ eV) and structure-sensitive ($\Delta E = 150$ eV) images that confirm peripheral staining of the primary DBS nanofibrils comprising the organogel network. Possible explanations for this observation are provided in the text. An electron-dense feature is circled as a reference marker in parts c and d.

dependent evolution of the dynamic elastic modulus (G') for four organogels heated to above the gel dissolution temperature (T_d) and then rapidly cooled to ambient temperature. Recall that these systems form physical gels, in which case G' is effectively independent of frequency (ω) and G' is always greater than the dynamic viscous modulus (G'').⁶³ For these reasons, the variation in G' is monitored in this and subsequent figures. As the DBS mass concentration (ϕ) is increased from 1.5 to 5.0 wt % DBS in Figure 3a, the rate at which G' increases is also observed to increase. According to these data, the gel time (t_g), taken here as the time required for G' to become constant, clearly decreases with increasing ϕ . Both observations regarding ϕ reflect the number density and, hence, relative proximity of DBS molecules available to participate in network formation.

A more rigorous protocol to extract t_g employs the Winter–Chambon criterion,^{64–66} which states that G''/G' becomes independent of ω at the gel point. By monitoring

the time variation of G''/G' at different frequencies, t_g can be identified as the point of common intersection. Although this methodology has been repeatedly found to yield reliable results, it is problematic with regard to the present DBS organogels due to a combination of shear sensitivity (gelation is slowed due to test-induced network damage) and fast gelation times (< 100 s at high ϕ). Another factor influencing t_g is matrix polarity, as evidenced in Figure 3b for organogels at a fixed concentration of 3 wt % DBS. In this case, the reduction in polarity achieved by methoxy end-group substitution systematically increases the rate at which G' increases, and decreases t_g in the order $t_g^{\text{PEGdme}} < t_g^{\text{PEGme}} < t_g^{\text{PEG}}$, at constant concentration and polymer molecular weight. These data confirm that the existence of polar end groups on a polymer chain can have a deleterious effect on the kinetics of gel formation, and they support our hypothesis that interactions between DBS molecules and hydroxyl end groups interfere with the self-organization of DBS molecules. Another feature of Figure 3 that warrants explanation is the presence of isolated spikes in G' at relatively high ϕ . These anomalies

(63) Kavanagh, G. M.; Ross-Murphy, S. B. *Prog. Polym. Sci.* **1998**, 23, 533.

(64) Chambon, F.; Petrovic, Z. S.; MacKnight, W. J.; Winter, H. H. *Macromolecules* **1986**, 19, 2146.

(65) Winter, H. H.; Chambon, F. *J. Rheol.* **1986**, 30, 367.

(66) Winter, H. H. *Polym. Eng. Sci.* **1987**, 27, 1698.

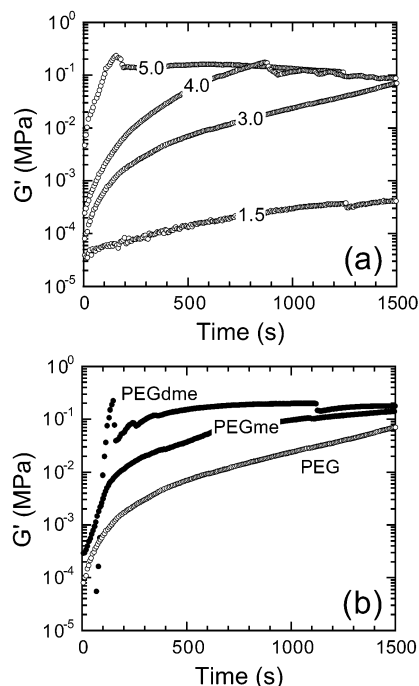


Figure 3. Time-dependent evolution of the dynamic elastic modulus (G') for (a) PEG/DBS organogels varying in DBS concentration (listed in wt %) and (b) organogels with 3 wt % DBS in PEG homopolymers differing in chain termination (identified in the figure). The strain amplitude and frequency are 1.5% and 10 rad/s, respectively.

can be attributed to either wall slip or transient structure failure during testing.

The time-dependent variation of G' in Figure 3b confirms the impact of end-group polarity on gel formation, which is believed^{27,67} to occur predominantly via intermolecular hydrogen-bonding between either neighboring hydroxyl groups or hydroxyl and acetal oxygen groups. Previous experimental results¹⁰ and current molecular dynamics simulations⁴⁴ also indicate that phenyl stacking may play a role in the self-organization of DBS. The effect of matrix polarity on network formation can likewise be probed by measuring the gel formation temperature (T_f) as the pregel solution is slowly cooled from temperatures above T_f . Values of G' measured from solutions with 5 wt % DBS cooled at a constant rate of 2 °C/min are shown as a function of temperature in Figure 4. Here, T_f is defined as the temperature at which G' abruptly increases, as illustrated in the figure. The order in which gelation is observed to occur is given by $T_f^{\text{PEGdme}} > T_f^{\text{PEGme}} > T_f^{\text{PEG}}$, which is consistent with the order of t_g listed above. While the t_g inferences afforded by Figure 3b are qualitatively useful, they are not subject to reliable and systematic quantitation. Values of T_f , on the other hand, can be readily extracted from the data provided in Figure 4 and are included in the inset. It is intriguing that T_f decreases (almost linearly) with increasing hydroxyl end-group number (n_{OH}) under the gel preparation conditions employed here. This unexpected result not only provides additional evidence for polarity-hindered network formation in this series of organogels, but also suggests that this effect is a direct consequence of the number density of hydroxyl groups in the organogels.

Fahrländer et al.² have also measured gel formation temperatures for PPG/DBS organogels in which the molecular weight of the PPG was varied. Our explanation

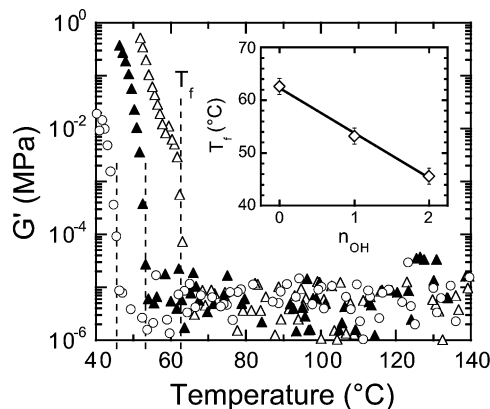


Figure 4. Dependence of G' on temperature at a cooling rate of 2 °C/min for 5 wt % DBS solutions differing in homopolymer matrix: PEG (○), PEGme (▲), and PEGdme (△). The strain amplitude and frequency are 1% and 10 rad/s, respectively. The gel formation temperature (T_f) is illustrated by the dashed vertical lines, and values of T_f are presented as a function of hydroxyl end-group number (n_{OH}) in the inset.

for the apparent variation of T_f with regard to PEG end-group functionality or, alternatively, matrix polarity in Figure 4 is consistent with their trends. Assuming that T_f effectively represents a freezing-point depression induced by the presence of polymer “solvent” molecules, they have adopted a regular solution model to extract a value of δ_{DBS} (23.9 J^{1/2}/cm^{3/2}) from their data. The magnitude of this value is reasonable in light of the apparent solubility of DBS in various organic solvents. The expression for T_f is written as

$$T_f = \frac{1 + \frac{v_{\text{ref}} v_{\text{DBS}} (\delta_p - \delta_{\text{DBS}})^2}{\Delta h_c v_p}}{1/T_c + R v_{\text{DBS}} / \Delta h_c v_p} \quad (2)$$

where v_i denotes the molar volume of species i (i = DBS or p for polymer), v_{ref} is a reference molar volume (taken as $\Phi_{\text{DBS}} v_{\text{DBS}} + \Phi_p v_p$, with Φ representing volume fraction), Δh_c is the heat of crystallization of pure DBS (32.2 kJ/mol),² T_c is the crystallization temperature of pure DBS, and R is the universal gas constant. Since the PEG end group varies in this work, v_p is not known a priori for each polymer species. To ascertain the molar volume and, hence, molecular weight of the polymer unit (M°) interacting with DBS to promote the measured depression in T_c , we have fitted eq 2 to the data in Figure 4. Using the value of δ_{DBS} reported by Fahrländer et al.² yields the following M° : 61 (PEG), 49 (PEGme), and 47 (PEGdme). As a basis, recall that the molecular weight of the CH₂CH₂O repeat unit is 44. Our result suggests that the effect of PEGdme on gel formation is similar to that of high-molecular-weight poly(ethylene oxide) (PEO) with a relatively low number of end groups. In other words, incorporating methoxy termination on PEG results in behavior similar to that of high-molecular-weight PEO, for which end-group effects are vanishingly small. On the other hand, the interaction unit of PEG is substantially larger and surprisingly comparable in magnitude to that of the ethylene glycol monomer (M° = 62). As anticipated, the value of M° for PEGme lies between those of PEG and PEGdme.

Now that we have established the importance of gel composition and matrix polarity on gel formation, we next turn our attention to the roles these factors play with regard to gel dissolution, which provides a direct measure of network stability. Figure 5a shows the dependence of G' on temperature as a series of PEG/DBS organogels

(67) Millner, E. O.; Titus, G. R. *Chem. Des. Autom. News* **1990**, 5, 1.

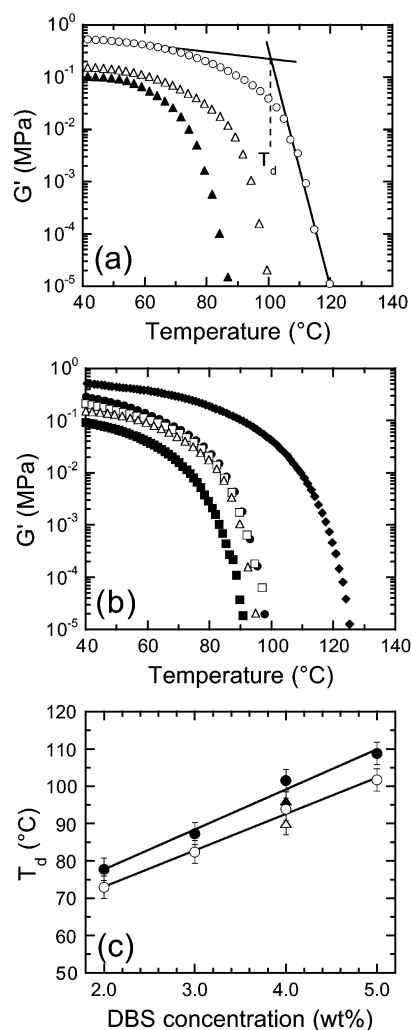


Figure 5. Elastic modulus provided as a function of temperature at a heating rate of 10 $^{\circ}\text{C}/\text{min}$ for (a) PEG/DBS organogels differing in DBS concentration (in wt %) [2 (\blacktriangle), 3 (\triangle), and 5 (\circ)] and (b) organogels with 3 wt % DBS in PEG homopolymers differing in chain termination [PEG (\triangle), PEGme (\square) and PEGdme (\bullet)]. Included for comparison in part b are data from PEGdme/DBS organogels with 2 (\blacksquare) and 5 (\blacklozenge) wt % DBS. The intersecting tangents used to identify the gel dissolution temperature (T_d) are illustrated in part a, and the dependence of T_d on DBS concentration in PEG (\circ) and PEGdme (\bullet) organogels is shown in part c. Included in part c are linear regressions to the data (solid lines), as well as additional data (PEG, \triangle ; PEGdme, \blacktriangle) collected at a slower heating rate (2 $^{\circ}\text{C}/\text{min}$). The strain amplitude and frequency are constant at 1% and 10 rad/s, respectively.

differing in ϕ from 2 to 5 wt % DBS are heated at a rate of 10 $^{\circ}\text{C}/\text{min}$. In all three cases, G' initially decreases slightly with increasing temperature. This reduction becomes more pronounced, until G' drops precipitously. Since this decrease in G' is not sharp, values of T_d are systematically identified by the intersection of the tangents drawn to the data at low and high temperatures, as depicted in Figure 5a. It is qualitatively evident from these data that T_d increases with increasing ϕ , indicating that more thermal energy is required to disrupt gel networks that contain more DBS molecules in a more densely packed arrangement of nanofibrils (see Figure 1c) at high DBS concentrations. A comparable trend, previously reported² for PPG/DBS organogels, is observed with regard to PEGdme in Figure 5b and is presented as a function of ϕ in Figure 5c. Parts b and c of Figure 5 reveal that T_d is only slightly dependent on matrix polarity.

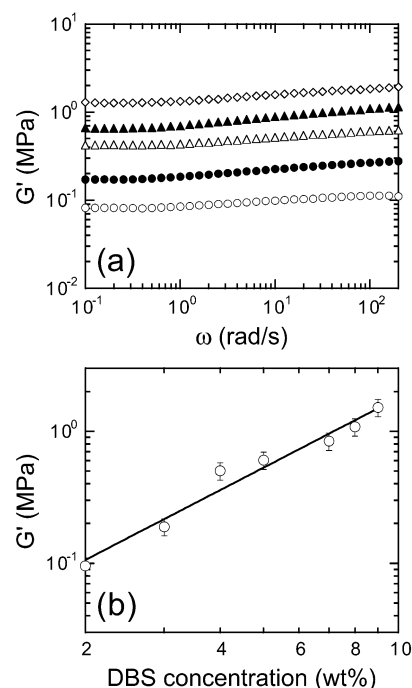


Figure 6. (a) Variation of G' with angular frequency (ω) for PEG/DBS organogels differing in DBS concentration (in wt %): 2 (\circ), 3 (\bullet), 4 (\triangle), 7 (\blacktriangle), and 9 (\diamond). (b) Mean values of G' presented as a function of DBS concentration on dual-logarithmic coordinates. The solid line in part b is a power-law fit to the data. The strain amplitude is 0.1%, and the temperature is 25 $^{\circ}\text{C}$.

While values of T_d are nearly indistinguishable for PEG, PEGme, and PEGdme in Figure 5b, they are more easily differentiated (within experimental uncertainty) for PEG and PEGdme in Figure 5c with the same result at different ϕ : $T_d^{\text{PEGdme}} > T_d^{\text{PEG}}$. Although a reduction in heating rate from 10 to 2 $^{\circ}\text{C}/\text{min}$ lowers T_d , the relative difference in T_d between PEG and PEGdme remains. These observations imply that the DBS network is marginally more stable in a nonpolar matrix than in a polar one, which explains why $T_d^{\text{PEGdme}} > T_d^{\text{PEG}}$ (see Figure 4).

Gel Microstructure and Activation Energy. Since the magnitude of G' provides a relative measure of network development in physical gels, it is therefore appropriate to examine the dependence of G' on DBS concentration. Frequency spectra of PEG/DBS organogels differing in ϕ are presented in Figure 6a and confirm that G' is independent of ω . Mean values of G' extracted from these data sets are shown as a function of DBS concentration in Figure 6b. According to this representation, G' (and the strength of the underlying DBS network) increases with increasing ϕ , exhibiting a power-law dependence of the form $G' \sim \phi^{1.8}$. While such a composition-induced increase in G' is entirely consistent with previous results obtained from both low-molar-mass^{26,27,30} and macromolecular^{2,3,16} organogels, it is curious that only this work and a previous study by McKenna and co-workers³⁰ report a scaling relationship between G' and ϕ . In our case, this relationship may be of limited value, however, since it is based on less than 1 order of magnitude in ϕ . Mercurio et al.¹⁶ have demonstrated that G' in PPG/DBS organogels increases sigmoidally, ultimately exhibiting a plateau, with increasing DBS concentration. The plateau is presumed to correspond to the range of ϕ over which the gel network becomes saturated with DBS molecules. It is reasonable to expect that, at higher ϕ than explored here, the gel network in PEG will likewise saturate and G' will

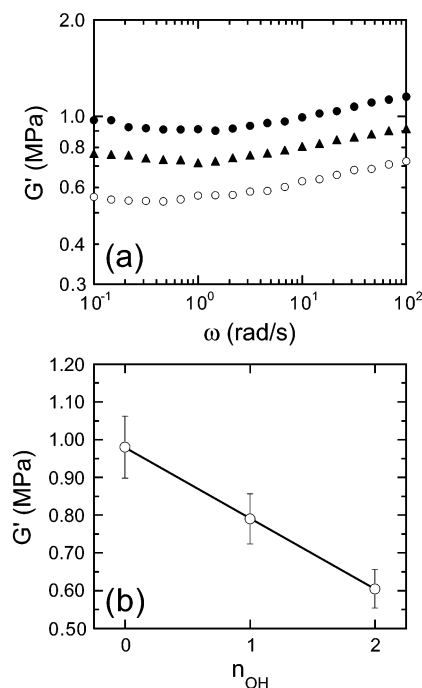


Figure 7. (a) Variation of G' with ω for organogels with 5 wt % DBS in PEG homopolymers differing in chain termination: PEG (○), PEGme (▲), and PEGdme (●). (b) Mean values of G' presented as a function of n_{OH} . The solid line in part b is a linear fit to the data. The strain amplitude is 0.1%, and the temperature is 25 °C.

also become independent of ϕ , although evidence of a G' plateau is presently unavailable.

Analogous results are displayed in Figure 7 for organogels differing in matrix polarity at a fixed concentration of 5 wt % DBS. Although the variation in G' among the three homopolymers is certainly less pronounced than that for the PEG/DBS organogels differing in ϕ in Figure 6, it is nevertheless discernible. Beyond experimental uncertainty, G' is found to decrease slightly with increasing hydroxyl density (n_{OH}). This observation is consistent with the gelation studies presented in Figures 3 and 4. At temperatures above T_d , the DBS molecules interact primarily with matrix molecules. As the solutions are cooled to below T_f , the DBS molecules self-organize, but at different rates and temperatures, depending on solvent polarity. While the DBS molecules may prefer to hydrogen-bond with each other, their bonding effectiveness is influenced by n_{OH} , in which case it is not surprising that the network formed (the slowest) in PEG is slightly less rigid due to considerable PEG–DBS interactions than the one formed (the fastest) in PEGdme with fewer PEGdme–DBS interactions. The corresponding difference in G' is not expected, or observed in Figure 7b, to be substantial if the gel network consists exclusively of stacked DBS molecules.¹⁰ We hasten to mention at this juncture that the values of G' reported in Figures 6 and 7 are slightly larger than those in the gelation tests (Figures 3 and 4) due to the shear sensitivity of DBS organogels, which tend to be damaged when continuously monitored (even using small-amplitude deformation) during gelation or postshear network recovery.¹⁶

The time–temperature superposition (tTS) methodology has been previously used² to ascertain an apparent activation energy (E_a) associated with network evolution in polyether organogels prepared with DBS. This approach greatly extends the range over which frequency or, alternatively, time is probed by collecting frequency

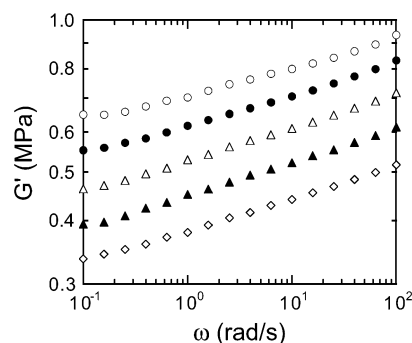


Figure 8. Frequency spectra of G' for PEG/DBS organogels with 5 wt % DBS measured at five different temperatures (in °C): 40 (○), 45 (●), 50 (△), 55 (▲), and 60 (◇). The strain amplitude is 0.5%.

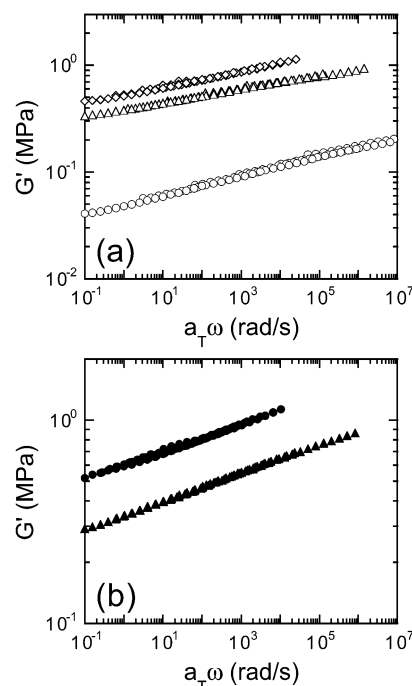


Figure 9. Representative master curves of G' provided as a function of temperature-shifted frequency ($a_T \omega$) for (a) PEG/DBS organogels differing in DBS concentration (in wt %) [3 (○), 5 (△), and 7 (◇)] and (b) organogels with 5 wt % DBS in PEG homopolymers differing in chain termination [PEGme (▲) and PEGdme (●)]. The strain amplitude is 0.5%.

spectra at different temperatures. To avoid complications due to gel dissolution at T_d , we have selected temperatures ranging from 30 to 60 °C for tTS. A representative example of temperature-consecutive frequency spectra acquired from a PEG/DBS organogel with 5 wt % DBS permitted to gel quiescently for 1 week (in contrast to the results shown in Figure 4 for gels cooled at 2 °C/min) is provided in Figure 8 and demonstrates that (i) the magnitude of G' is sensitive to gel formation/recovery time^{16,68} and (ii) an increase in temperature promotes a systematic reduction in G' over the entire ω range examined. The spectra corresponding to temperatures below 60 °C are then shifted along the frequency axis until they align to generate master curves, which are shown for PEG/DBS organogels differing in ϕ in Figure 9a, as well as for PEGme/DBS and PEGdme/DBS organogels in Figure 9b. The quality of these master curves, signified by how well the data fit to form a smooth curve, provides an immediate indication of

(68) Wilder, E. A.; Hall, C. H.; Spontak, R. J. *J. Colloid Interface Sci.* (submitted).

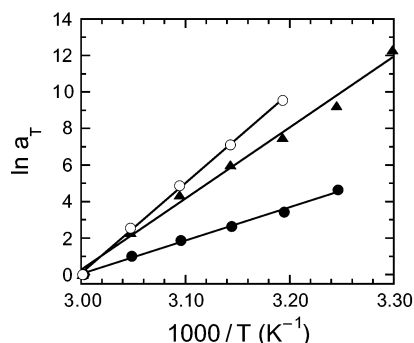


Figure 10. Temperature shift factors (a_T) for a PEG/DBS organogel with 5 wt % DBS (\circ) and two PEGdme/DBS organogels with 2 (\blacktriangle) and 5 (\bullet) wt % DBS presented as functions of reciprocal temperature. The solid lines correspond to fits of the Arrhenius equation (eq 3 in the text).

whether the tTS protocol can be applied to these systems. Applicability of tTS constitutes an important consideration, since Fahrlander et al.⁶⁹ have recently found that this analysis strategy does not accurately describe organogels composed of a barbituric acid/2,4,6-triaminopyrimidine gelator in isotactic and atactic polypropylene. The data provided in Figure 9, however, confirm that the temperature-dependent $G'(\omega)$ spectra of all the DBS-containing organogels investigated here can be smoothly shifted with respect to ω to produce well-behaved master curves. Similar behavior is also observed for the $G''(\omega)$ spectra (data not shown).

Another important consideration in tTS is the functionality of the shift factor (a_T), which should vary monotonically with temperature. If the response of the gel network to temperature is thermally activated, the temperature dependence of a_T can be used to extract information regarding E_a through an Arrhenius equation of the form

$$a_T = K e^{E_a/RT} \quad (3)$$

where K is a constant and T denotes absolute temperature. The temperature dependence of a_T (with 60 °C arbitrarily chosen as the reference temperature so that $a_{60\text{ °C}} = 1$) is illustrated for three organogels in Figure 10 and verifies that the shift factor exhibits Arrhenius behavior in these organogels. Quantitatively similar results are likewise obtained from $G'(1/T)$ at any given ω . This observation confirms that the DBS network forms by a thermally activated mechanism, which agrees with the previous results of Fahrlander et al.² and Mercurio and Spontak¹⁶ for PPG/DBS organogels, and suggests that this aspect of DBS-containing organogels may, in fact, be general. Using a combination of light scattering and dynamic rheology, Liu and Sawant^{70,71} have likewise reported that organogels composed of *N*-lauroyl-L-glutamic acid di-*n*-butylamide in isostearyl alcohol form by thermally activated nucleation and growth. Values of E_a extracted from the $a_T(T)$ data generated during tTS are presented as functions of DBS concentration for PEG/DBS organogels in Figure 11a and solvent polarity (n_{OH}) in Figure 11b.

Figure 11a clearly reveals that E_a decreases (linearly) with increasing ϕ , which, together with the data in Figure 3a, provides further evidence that network evolution becomes increasingly more facile as ϕ is increased.

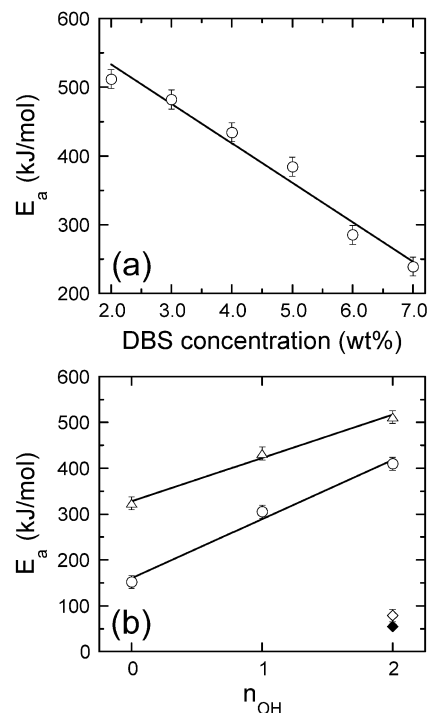


Figure 11. Activation energy (E_a) values derived from the temperature dependence of a_T (see Figure 10) for (a) PEG/DBS organogels differing in DBS concentration and (b) organogels in PEG homopolymers differing in chain termination at two DBS concentrations (in wt %): 2 (Δ) and 5 (\circ). The solid lines in both figures are linear fits to the data. Included in part b are E_a values for PPG/DBS organogels with 0.4 wt % DBS reported by Fahrlander et al.² (\blacklozenge) and measured in this work (\diamond). The error bars correspond to one standard deviation in the data.

Conversely, the energy barrier that must be overcome for the DBS molecules to form a percolated nanofibrillar network increases with decreasing ϕ . A similar conclusion has been previously reached¹⁶ with regard to DBS/PPG organogels on the basis of temperature-dependent spectrophotometric results. In the present work, values of E_a decrease by more than 50%, from 512 to 239 kJ/mol, as ϕ increases from 2 to 7 wt % DBS. In Figure 11b, E_a is observed to increase linearly with increasing matrix polarity for two series of organogels differing in ϕ . These combined results indicate that the self-organization of DBS molecules into a network structure becomes more energetically favored as the DBS concentration is increased and the matrix polarity is reduced. This conclusion is supported by the findings of Yamasaki and Tsutsumi,²⁶ who demonstrated that bonding between DBS molecules increases as solvent polarity decreases in DBS-containing organogels composed of low-molar-mass organic solvents. Under these conditions, DBS molecules interact relatively little with the matrix molecules, thereby facilitating network formation and gelation (see Figure 3b). At a DBS concentration of 5 wt %, the extracted values of E_a for PEG, PEGme, and PEGdme are 410, 305, and 152 kJ/mol, respectively.

These activation energies are, however, substantially higher than the value of E_a (55 kJ/mol) reported by Fahrlander et al.² for PPG/DBS organogels ($\bar{M}_n = 5150$) with 0.4 wt % DBS. Since PPG is a less polar molecule than any of the PEG derivatives examined in this study due to the presence of an additional methyl group per repeat unit, a reduction in E_a is certainly reasonable in light of the findings included in Figure 11b. That is, the DBS molecules should interact (via hydrogen bonding)

(69) Fahrlander, M.; Fuchs, K.; Mülhaupt, R.; Friedrich, C. *Macromolecules* (submitted).

(70) Liu, X. Y.; Sawant, P. D. *Appl. Phys. Lett.* **2001**, *79*, 3518.

(71) Liu, X. Y.; Sawant, P. D. *Adv. Mater.* **2002**, *14*, 421.

less with the PPG molecules than with PEGdme molecules, thereby improving the likelihood of DBS–DBS interactions and subsequent self-organization of DBS into a percolated network at sufficiently high ϕ in a PPG matrix. This expectation is reflected in the minimum DBS concentration required to induce physical gelation (ϕ^*). In the case of PPG, ϕ^* is typically less than 0.7 wt % DBS (decreasing with increasing \bar{M}_n) due to little interaction between DBS and PPG molecules,¹⁶ but increases to more than 1 wt % DBS in PEG and its end-group-modified derivatives. To determine if the calculated E_a values displayed in Figure 11b are consistent with the activation energy reported² for PPG from tTS, we have examined a PPG/DBS organogel ($\bar{M}_n = 1000$) at a concentration of 0.5 wt % DBS. In this case, E_a is about 79 kJ/mol, which is in fair agreement with the result of Fahlränder et al.² From the measured dependence of ϕ^* on \bar{M}_n observed by Mercurio et al.,¹⁶ however, we anticipate that E_a will decrease with increasing \bar{M}_n in PPG as a consequence of the accompanying reduction in matrix polarity (due to the decrease in the hydroxyl number density, ϵ).

Conclusions

Dibenzylidene sorbitol is a low-molar-mass organic gelator that self-organizes on the molecular level and physically gels a wide variety of macromolecules, including poly(ethylene glycol) (PEG) and two of its chemical derivatives differing in termination, at relatively low concentrations. The gel networks produced in this work consist of nanofibrils measuring between about 10 and 70 nm in diameter, which is consistent with results obtained for DBS in other organic solvent and polymer systems. Selectively stained specimens reveal the existence of a “primary” nanofibril with a diameter of ~ 10 nm. An increase in the concentration of DBS is observed to promote an increase in the rate of gelation, as well as in the magnitude of the elastic modulus and the temperature

stability of PEG/DBS organogels. By systematically varying the chemical nature of the end groups on PEG from polar (hydroxy-endcapped) to nonpolar (methoxy-endcapped), we have demonstrated that matrix polarity has a deleterious effect on DBS/PEG gelation. In a polar medium, the rate at which DBS self-organization, and hence gelation, proceeds slows down due to competing interactions with matrix molecules. This effect also reduces the gel formation and dissolution temperatures. Matrix polarity appears to impact only the gel formation (or dissolution) process, since it does not appear to influence the magnitude of the equilibrium modulus ultimately achieved by a gel at a given DBS concentration. Time–temperature superposition analysis has been conducted on these gels and reveals that the temperature shift factor exhibits Arrhenius behavior, thereby confirming that gelation occurs by a thermally activated mechanism. Values of the activation energy are sensitive to both DBS concentration and matrix polarity. As the DBS concentration is increased and the number density of DBS molecules available to self-organize into a network likewise increases, the activation energy for gelation decreases. Similarly, gels prepared in a polar matrix possess higher activation energies than those in nonpolar matrices, which can again be attributed to interactions between DBS and polar matrix molecules. These findings provide valuable insight into the fundamental factors governing the gelation process of DBS and indicate that DBS molecules can interact with matrix molecules during gelation, but ultimately prefer to self-organize with other DBS molecules.

Acknowledgment. E.A.W. thanks the Eastman Chemical Co. and the North Carolina Space Grant Consortium Program at NC State University for graduate research fellowships.

LA027081S